phys. stat. sol. (c) **4**, No. 11, 4049–4053 (2007) / **DOI** 10.1002/pssc.200675901

Magnetic properties of multiferroic $TbMnO_3$ doped with Al

F. Pérez[1], **J. Heiras**[*1], and **R. Escudero**[2]

[1] Centro de Ciencias de la Materia Condensada, Universidad Nacional Autónoma de México, Km. 107.5 Carretera Tijuana-Ensenada, Ensenada, B.C., México
[2] Instituto de Investigaciones en Materiales, Universidad Nacional Autónoma de México, A. Postal 70-360, México, D.F. 04510, Mexico

Received 16 October 2006, revised 6 March 2007, accepted 30 May 2007
Published online 26 October 2007

PACS 75.47.Lx, 75.50.Ee

The synthesis, characterization, and magnetic properties of polycrystalline $Tb_{1-x}Al_xMnO_3$ with x = 0.05 and 0.1 is reported. Samples were synthesized by the conventional solid state reaction method producing single phase compounds. Rietveld refinements indicate that Al substitutes Tb in the structure. Samples were highly porous with grain sizes up to ~10 μm. The magnetic measurements show a magnetic ordering, starting from antiferromagnetism, for the undoped sample, to a weak ferromagnetic phase coexisting with the antiferromagnetic phase for the two x values. The magnetic ordering is attributed to two different contributions of Mn and Tb sublattices.

1 Introduction

Materials with perovskite related structure, like manganites, possess a great variety of physical properties important for new technological developments. Their potential applications in information storage, spintronics, sensors and new novel devices demand an intensive investigation [1]. Properties such as the multiferroic behavior [2], in which ferroelectricity and magnetic order occur on the same phase, have been recently revealed in the perosvskite compound TbMnO3 [3, 4]. Much of the studies in the multiferroic $TbMnO_3$ have been performed in single crystals, and reports on polycrystalline nanoparticles have been scarce [5, 6]. Such manganites present a distorted perovskite structure, which is closely related to the magnetic properties [7–12]. Studies in more complex compounds like $R_{1-x}A_xMnO_3$ (R = rare earth; A = Ba, Sr, Ca) present a wide variety of magnetic structures [13, 14], and charge ordering [15, 16]. In this article we report the synthesis, characterization, and the magnetic properties of the compound $Tb_{1-x}Al_xMnO_3$ prepared by the conventional solid state reaction method.

2 Experimental

A set of $Tb_{1-x}Al_xMnO_3$ samples (with x = 0, 0.05, 0.1) were synthesized by solid state method. Stoichiometric amounts of Tb_4O_7, MnO_2, and Al_2O_3 powders with high purity, 99% and 99.99%, were mixed and grounded in an agate mortar for about 1 h approximately. Pelletized samples with the mixed powders were obtained by pressed at 5000 kPa and sintered at 1200 ^oC in air for 12 h, with a slow heating ramp. X-ray diffraction (XRD) powder analysis was performed in a Philips diffractometer model X'Pert with Cu K_α radiation. In order to perform the Rietveld analysis, the X-ray measurements were scanned from $5^o < 2\theta < 120^o$ in 0.02^o steps, for 8 h. Structural refinements were performed using a FULL-

[*] Corresponding author: e-mail: heiras@ccmc.unam.mx

PROF program [17]. Samples also were characterized by electron dispersive spectroscopy analysis (EDS), and surface morphology by scanning electron microscopy (SEM), with a microscope JEOL JSM-5300. The magnetization measurements were acquired using a Quantum Design SQUID Magnetometer model MPMS-5S.

3 Results and discussion

Figure 1(a) presents the XRD pattern for the polycrystalline $TbMnO_3$ sample at room temperature. It coincides well with the data base for the orthorhombic $TbMnO_3$ phase [ICDD 25-0933]. Determined unit cell parameters were: a = 5.29 Å, b = 5.83 Å, and c = 7.40 Å. Figure 1(b) shows de XRD patterns for the compounds $Tb_{1-x}Al_xMnO_3$ with x = 0.05, and 0.1, the patterns were compared to the $TbMnO_3$ phase. This figure demonstrates that these compounds present the same crystalline structure as the $TbMnO_3$ phase, with only small variation due to the Al metal substitution. There are not observable second or segregate phases.

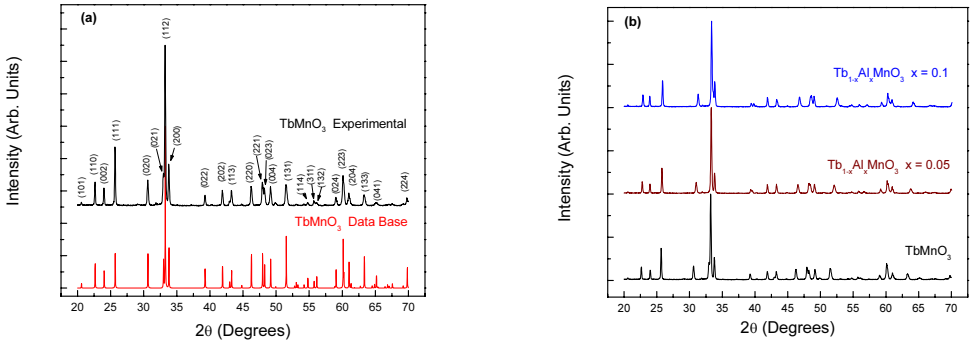

Fig. 1 XRD powder patterns for (a) pure $TbMnO_3$ and (b) doped $Tb_{1-x}Al_xMnO_3$ with x = 0.05 and 0.1.

Rietveld refinements shown in Figs. 2a and 2b, allowed a precise calculation of the unit cell parameter. The *c* parameter increases, while *a* and *b* decrease. This is depicted in Table 1. This behavior is similar of those found in related perovskites [10]. The cell volume decreases according with aluminum concentration, because the size of Al^{3+} ions is approximately half size small than Tb^{3+} ions in the same coordination. It is important to mention that Rietveld refinements, assuming that Al atoms were in the Mn site, instead of Tb site, do not converged for Al concentrations higher than 0.1. It suggests that Al atoms substitute Tb, as was initially planned.

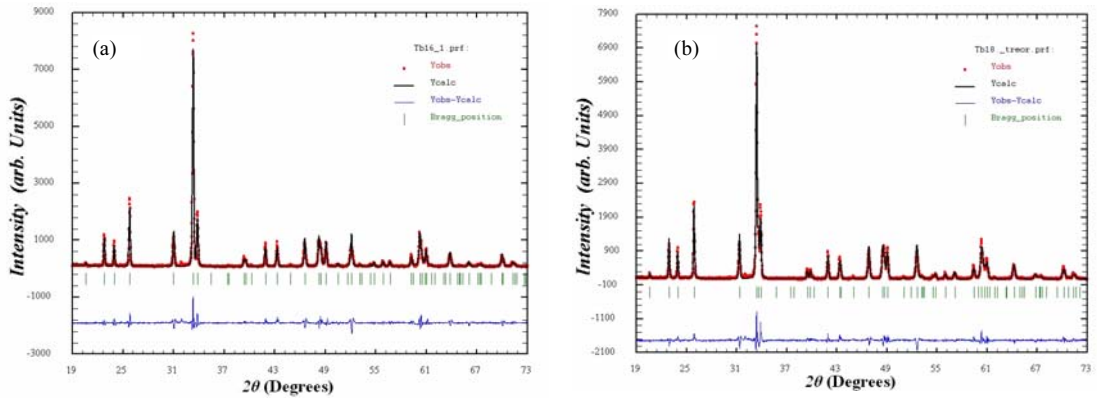

Fig. 2 Rietveld refinements of the X-ray diffraction data at room temperature for (a) $Tb_{.95}Al_{.05}MnO_3$ and (b) $Tb_{.9}Al_{.1}MnO_3$.

Table 1 Lattice parameters and unit cell volume for $Tb_{1-x}Al_xMnO_3$ samples at room temperature.

Lattice parameter	$TbMnO_3$ (Å)	$Tb_{.95}Al_{.05}MnO_3$ (Å)	$Tb_{.9}Al_{.1}MnO_3$ (Å)
a	5.297	5.2909	5.2829
b	5.831	5.7592	5.7008
c	7.403	7.4155	7.4190
Unit cell volume ($Å^3$)	228.494	225.965	223.440

Scanning electron micrograph for these compounds is illustrated in Fig. 3a. This shows the grain size dimensions oscillating from less than 1 μm to about ~10 μm. In Fig. 3b the electron dispersive analysis confirmed the presence of the expected elements and no contamination impurities were found.

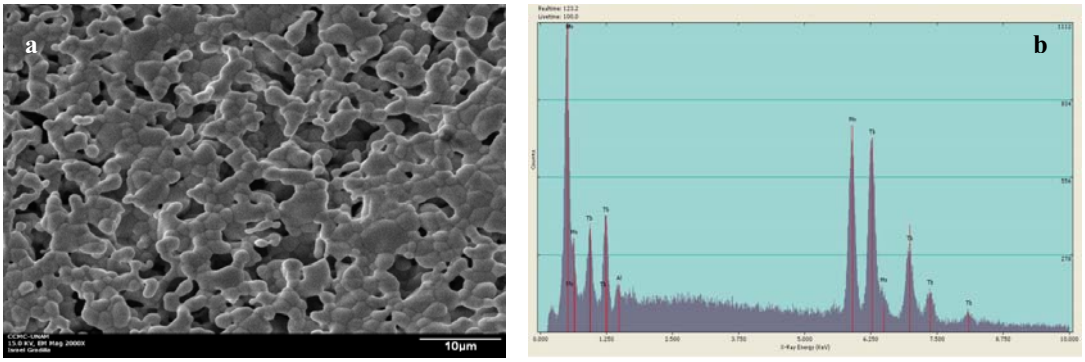

Fig. 3 (a) Scanning electron micrograph, and (b) electron dispersive spectrum for the polycrystalline $Tb_{.95}Al_{.05}MnO_3$.

Figure 4a shows the temperature dependence of the magnetization, M(T), in zero field cooling mode (ZFC) for the samples with composition; x = 0, 0.05, 0.1. As is well known single phase polycrystalline samples of $TbMnO_3$ compound presents an antiferromagnetic (AF) transition at about 10 K [6]; this is consistent with our data as shown in the insert of Fig. 4a. The substitution of Tb by Al changes drastically M(T). In Fig. 4a, a huge magnetization increase is observed for the doped samples. Very small amounts of Al (x = 0.05) change the magnetic order from AF to a weak ferromagnetism. However, as Al is increased to x = 0.1, a peak in the magnetization is observed at about 33 K. This characteristic can be explained assuming that the crystalline structure presents canted spins, thus two magnetic ordering, AF and weak ferromagnetism, persist. The Curie temperature for both compositions is close to 45 K. Figure 4b depicts clearly this weak ferromagnetic effect. Here the sample with x = 0.1 was measured at two magnetic field intensities. At 1 kOe the ZFC and field cooling (FC) measurements have a rather small irreversibility below 5 K which is not appreciated in the figure. However at 5 kOe the irreversibility is now quite notorious for two reasons: the maximum is decreased at 22 K, and the irreversibility is at 30 K. High magnetic field intensities will present only a ferromagnetic behavior without irreversibility, as is normally observed in weak ferromagnetic systems. It is important to mention that in a perfect AF system the ZFC and FC measurement modes never show irreversibility. However an imperfect spin antiparallel alignment shows the irreversibility as in Fig. 4b. This irreversibility at high intensities of magnetic field will decrease, and eventually the M-T characteristic will be quite similar to a ferromagnetic material, but with a smaller magnetization than for a normal strong ferromagnetic material.
Isothermal magnetization measurements M(H) Figures 5a and 5b present a big coercive field, indicative that for these compositions, both ferromagnetism and antiferromagnetism could be coexisting, and that canted spins are influencing the magnetic behavior.

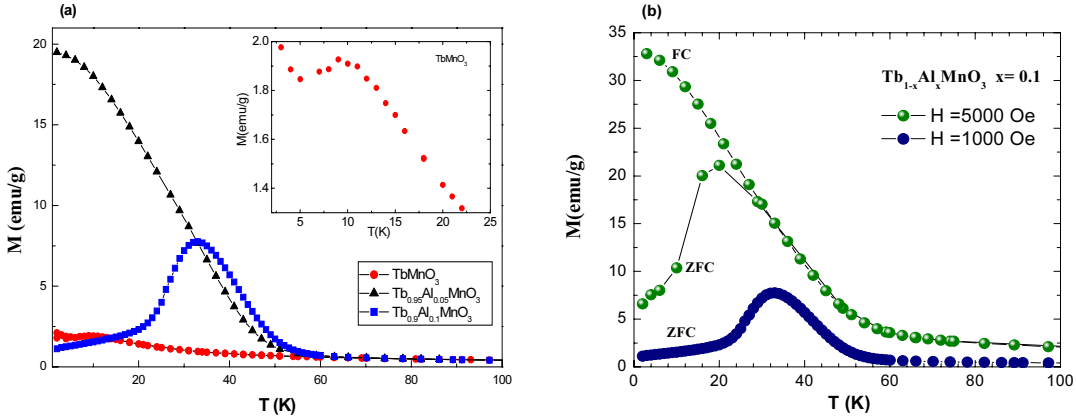

Fig. 4 a) ZFC magnetization M(T) for $TbMnO_3$ and $Tb_{1-x}Al_xMnO_3$ with x = 0.05, 0.1 at H = 1000 Oe. b) M(T) for sample with x = 0.1 at two magnetic fields. Note the irreversibility at 5 kOe which is indicative of a weak ferromagnetic coupling due to canted spins.

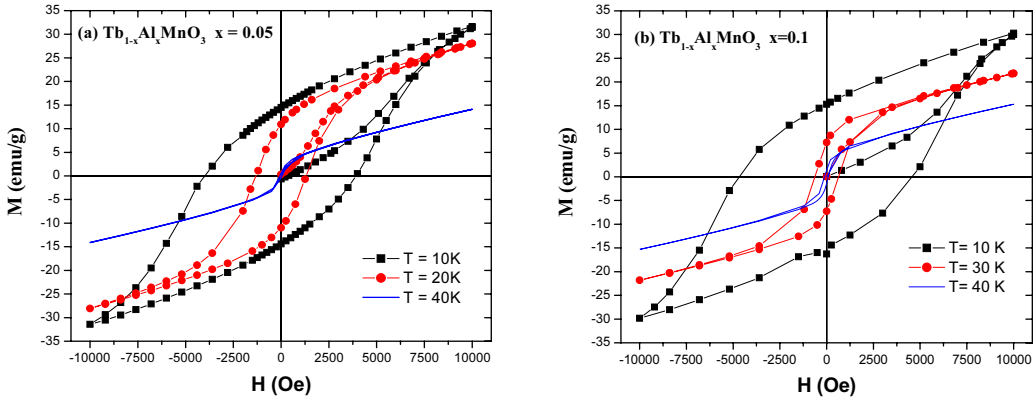

Fig. 5 (a) Hysteresis loops for the compound $Tb_{.95}Al_{.05}MnO_3$ at temperatures T = 10, 20, and 40 K. (b) Hysteresis loops for the compound $Tb_{.9}Al_{.1}MnO_3$ at temperatures T = 10, 30, and 40 K.

The samples follow the Curie-Weiss law at high temperatures. Plots of χ^{-1} vs T for x = 0 and x = 0.1 are shown in Fig. 6. $TbMnO_3$ follows the Curie-Weiss law down to ~45 K due to the ordering of Mn magnetic moments as was reported by J. Blasco *et al.* [10]. The other sample, x = 0.1, follows Curie behavior down to ~70 K. Using the Curie-Weiss susceptibility law, $\chi = C/(T-\theta)$, we obtained the effective magnetic moments μ_{eff} (μ_B) from the slope of the fitted straight lines. The obtained values for μ_{eff} are close to the value for Tb^{3+} of 9.5μ_B (see Table 2).

Table 2 Magnetic constants, experimental effective magnetic moments (Bohr magneton per formula unit) and the fit range of the susceptibility. data for selected samples.

Sample	*C* (emu K/mol)	μ_{eff} (μ_B)	Fitting range
$TbMnO_3$	14.28	10.68	45-300 K
$Tb_{0.9}Al_{0.1}MnO_3$	13.22	10.28	70-300 K

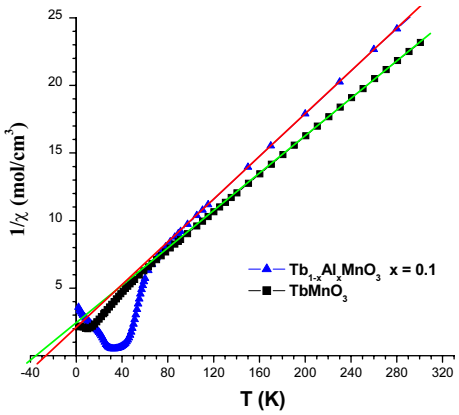

Fig. 6 Inverse of the magnetic susceptibility versus temperature for $Tb_{1-x}Al_xMnO_3$ with x = 0 and 0.1 samples fitted to Curie-Weiss law with straight lines from high temperatures.

4 Conclusions

This work presents our results of studies in single phase polycrystalline $TbMnO_3$ (pure and doped) samples obtained by the solid state reaction method. Two synthesized doped samples with Al substituting Tb, were indexed. Rietveld refinements results show that the aluminium is introduced into the Tb sites. Doping with Al produces changes in the magnetic ordering. Doped samples show a weak ferromagnetic behavior coexisting with an antiferromagnetic order, due to canted spins. This complex magnetic order observed can be attributed in principle, to the ordering of Tb^{3+} magnetic moments.

Acknowledgements We want to thank to P. Casillas, I. Gradilla, E. Aparicio, L. Baños, M. Castellanos for the technical support. Fruitful discussions with A. Durán are gratefully acknowledged. Finally, we thank for the support received from PAPIIT (DGAPA-UNAM) Proy. No. IN116703, IN100903 and by CONACyT Proy. No. 40604-F, 47714-F.

References

[1] J. F. Scott, Mater. Sci. Eng. B **120**, 6–12 (2005).
[2] W. Eerenstein, N. D. Mathur, and J. F. Scott, Nature **442**(17), 759–765 (2006).
[3] T. Kimura, H. Shintani, K. Ishizaka, T. Arima, and Y. Tokura, Nature **426**, 55–58 (2003).
[4] N. Hur, S. Park, P. A. Sharma, J. S. Ahn, S. Guha, and S-W. Cheong, Nature **429**, 392–395 (2004).
[5] S. Kharrazi, D. C. Kundaliya, S. W. Gosavi, S. K. Kulkami, T. Venkatesan, S. B. Ogale, J. Urban, S. Park, and S.-W. Cheong, Solid State Commun. **138**, 395–398 (2006).
[6] Yimin Cui, Liuwan Zhang, Guanlin Xie, and Rongming Wang, Solid State Commun. **138**(10–11), 481–484 (2006).
[7] T. Kimura, S. Ishihara, H. Shintani, T. Arima, K. T. Takahashi, K. Ishizaka, and Y. Tokura, Phys. Rev. B **68**, 060403 (2003).
[8] R. Kajimoto, H. Yoshizawa, H. Shintani, T. Kimura, and Y. Tokura, Phys. Rev. B **70**, 012401 (2004).
[9] S. Quezel, F. Tcheou, J. Rossat-Mignot, G. Quezel, and E. Roudaut, Physica B **86-88**, 916–918 (1977).
[10] J. Blasco, C. Ritter, J. García, J. M. de Teresa, J. Pérez-Cacho, and M. R. Ibarra, Phys. Rev. B **62**(9), 5609–5618 (2000).
[11] Y. H. Huang, H. Fjellvag, M. Karppinen, B. C. Hauback, H. Yamauchi, and J. B. Goodenough, Chem. Mater. **18**, 2130–2134 (2006).
[12] T. Kimura, G. Lawes, T. Goto, Y. Tokura, and A. P. Ramirez, Phys. Rev. B **71**, 224425 (2005).
[13] J. E. O. Wollan and W. C. Koehler, Phys. Rev. **100**, 545–563 (1955).
[14] Z. Jirák, S. Kupricka, Z. Simsa, M. Dlouhá, and S. Vratislav, J. Magn. Magn. Mater. **53**, 153–159 (1985).
[15] C. N. R. Rao, A. K. Cheetham, and R. Mahesh, Chem. Mater. **8**, 2421–2425 (1996).
[16] R. Kajimoto, H. Yoshizawa, H. Kawano, H. Kuwara, Y. Tokura, K. Ohayama, and M. Ohashi, Phys. Rev. B **60**, 9506–9517 (1999).
[17] J. Rodriguez-Carvajal, FULLPROF: A Program for Rietveld Refinement and Pattern Matching Analysis, Abstracts of the Satellite Meeting on Powder Diffraction of the XV Congress of the IUCr, Toulouse, France 1990, p. 127.